High-resolution energy-selected study of the reaction $CH_3X^+ \rightarrow CH_3^+ + X$: Accurate thermochemistry for the CH_3X/CH_3X^+ (X=Br, I) system

Y. Song, X.-M. Qian, K.-C. Lau, and C. Y. Ng[a)]
Ames Laboratory, U.S. Department of Energy, Ames, Iowa 50011
and Department of Chemistry, Iowa State University, Ames, Iowa 50011

Jianbo Liu and Wenwu Chen
Lawrence Berkeley National Laboratory, Chemical Science Division, Berkeley, California 94720

(Received 21 February 2001; accepted 19 June 2001)

Using the high-resolution pulsed field ionization-photoelectron (PFI-PE) and PFI-PE-photoion coincidence (PFI-PEPICO) techniques, we have examined the formation of methyl cation (CH_3^+) from the dissociation of energy-selected CH_3X^+ (X=Br and I) near their dissociation thresholds. The breakdown diagrams for CH_3X thus obtained yield values of 12.834±0.002 eV and 12.269±0.003 eV for the 0 K dissociative threshold or appearance energy (AE) for CH_3^+ from CH_3Br and CH_3I, respectively. Similar to the observation in PFI-PE studies of CH_4, C_2H_2, and NH_3, the PFI-PE spectrum for CH_3Br exhibits a step at the 0 K AE for CH_3^+, indicating that the dissociation of excited CH_3Br in high-n ($\geqslant$100) Rydberg states at energies slightly above the dissociation threshold occurs in a time scale of $\leqslant 10^{-7}$ s. The observed step is a confirmation of the 0 K AE(CH_3^+) from CH_3Br determined in the PFI-PEPICO study. The adiabatic ionization energies (IEs) for the $CH_3Br^+(\tilde{X}\,^2E_{3/2,1/2})$ spin–orbit states were determined by PFI-PE measurements to be 10.5427±0.0010 and 10.8615±0.0010 eV, respectively, yielding the spin–orbit coupling constant to be 2571±4 cm^{-1}. The AE(CH_3^+) values from CH_3Br and CH_3I and the IE[$CH_3Br^+(\tilde{X}\,^2E_{3/2})$] value obtained here, when combined with the known IE of CH_3 (9.8380±0.0004 eV) and IE[$CH_3I^+(\tilde{X}\,^2E_{3/2})$] (9.5381±0.0001 eV), have allowed accurate determination of the 0 K bond dissociation energies for CH_3–Br (2.996±0.002 eV), CH_3^+–Br (2.291±0.002 eV), CH_3–I (2.431±0.003 eV), and CH_3^+–I (2.731±0.003 eV). Using the AE(CH_3^+) from CH_3Br and CH_3I, together with the known 0 K heats of formation ($\Delta_f H_0^0$) for Br (117.93±0.13 kJ/mol), I (107.16±0.04 kJ/mol), and CH_3^+ (1099.05±0.33 kJ/mol), we have obtained more precise $\Delta_f H_0^0$ values for CH_3Br (−21.30±0.42 kJ/mol) and CH_3I (22.43±0.50 kJ/mol). This experiment demonstrated that highly reliable $\Delta_f H_0^0$ values for a range of molecules with error limits comparable to those for some of the most precisely measured values, such as $\Delta_f H_0^0(CH_4)$, can be obtained by PFI-PE and PFI-PEPICO measurements. © *2001 American Institute of Physics.*
[DOI: 10.1063/1.1391268]

I. INTRODUCTION

Reliable predictions of chemical reactivity require accurate energetic information for a broad range of molecular species. For this reason, to establish an accurate thermochemical database for molecules has been a major pursuit of both experimental and theoretical research in physical science.[1–3] The photoionization techniques based on the detection of photoelectrons and photoions have a distinguished history in providing reliable energetic information for molecules and their ions.[4] Important energetic data obtainable from photoionization experiments include ionization energies (IEs) and 0 K dissociative photoionization thresholds or appearance energies (AEs) of molecules, from which 0 K bond dissociation energies (D_0's) and 0 K heats of formation ($\Delta_f H_0^0$) for the neutral and ionic species can be derived by using appropriate thermochemical cycles. In conventional photoelectron spectroscopy and photoionization efficiency (PIE) studies, the error limits for measured energetic data are generally in the range of 1.3–8.4 kJ/mol.[1–3] Considering that photoelectron spectroscopy and photoionization efficiency (PIE) measurements are gas phase techniques and work well for relatively small molecules, we believe that a realistic goal of these photoionization experiments should be to build the best possible energetic data set for guiding the development of quantum chemical computation procedures.[5,6] The establishment of reliable computation codes would then allow the prediction of energetic properties for molecular species that are not accessible to experimental investigations.

Experimental energetic data for small molecules, including those obtained in photoionization experiments, have indeed played an essential role in the development of quantum chemical computation procedures.[5,6] Due to the advance in computer technologies, significant progress has been made in computation chemistry in the past decade. Currently, the

[a)]Author to whom correspondence should be addressed. Electronic mail: cyng@ameslab.gov

Gaussian-2/Gaussian-3 (G2/G3) procedures[5,6] are among the most popular quantum chemical computation schemes for energetic calculations. These theories are ''slightly'' semiempirical in nature because they contain a high level correction obtained empirically from a fit to a set of experimental energetic data, such as IEs, electron affinities, and heats of formation, by minimizing the deviations between corresponding experimental and theoretical results. The G2 theory[5] uses a data set of 55 molecules as compared to the use of a larger set of 299 molecules in the fitting for the G3 procedures.[6] As a result, the accuracy of G2/G3 predictions is dictated by error limits of experimental data used in the fitting. At present, the G2/G3 predictions for IEs, electron affinities, and heats of formation for small main group molecular species are known to achieve an accuracy of $\approx$3.8–5.4 kJ/mol as measured by the average deviations between theoretical and experimental results.[5,6] Without doubt, the development of the next generation of computation procedures would demand a more accurate experimental database.

The fact that standard computation codes can now achieve experimental accuracy has set a challenge for modern photoionization studies. The recent introduction of an array of pulsed field ionization (PFI) techniques, involving PFI-photoelectron (PFI-PE),[7–9] PFI-photoion,[10] and PFI-ion-pair[11] detection using lasers[9] and high-resolution monochromatized vacuum ultraviolet (VUV) synchrotron radiation,[12–14] have greatly improved the achievable energy resolution for photoionization measurements. These PFI studies have shown to provide IE values with error limits about 10–100-fold smaller than those observed in conventional photoelectron and PIE studies.[9] The recent implementation of a high-resolution synchrotron based PFI-PE-photoion coincidence (PFI-PEPICO) method has made possible the examination of unimolecular dissociation reactions of ions with an internal energy selection of 0.6–1.0 meV [full width at half maximum (FWHM)], limited only by PFI-PE measurements. Furthermore, we have discovered that 0 K AEs for dissociative photoionization processes involving a range of molecules can be identified by a sharp step resolved in the PFI-PE spectrum.[15,16] The origin of this step is attributed to the lifetime switching effect at the 0 K AE, where excited parent molecules in high-n ($n \geqslant 100$) Rydberg states with shorter lifetimes are converted into excited fragments in high-n ($n \geqslant 100$) Rydberg states with longer lifetimes.[15] The measurement of breakdown curves for the parent and daughter ions in PFI-PEPICO measurements, together with the observation of the PFI-PE step, has yielded highly reliable 0 K AE values for a range of molecules achieving error limits of about ± 0.001 eV (0.10 kJ/mol).[16–18] The 0 K AE values obtained in PFI-PE and PFI-PEPICO measurements have made possible the determination of 0 K dissociation energies (D_0's), and 0 K heats of formation ($\Delta_f H_0^0$'s) for many neutrals and ions with unprecedented precision.[16–18] These 0 K energetic values, which measure differences between well defined molecular energy levels, are most appropriate for direct comparison with theoretical calculations. We note that many energetic data for molecular species in the literature were obtained by equilibrium and kinetic measurements with temperatures well above 0 K.

We have employed the PFI-PE and PFI-PEPICO methods for investigating the photoionization and dissociative photoionization of a series of small molecules, such as CH_4, C_2H_2, C_2H_4, NH_3, C_2H_5Cl, C_2H_5Br, C_3H_7Cl, C_3H_7Br, and C_3H_7I, with excellent results.[15–20] We found that the uncertainties of some $\Delta_f H_0^0$ values for the radicals and ion fragments derived from these studies, such as CH_3 and CH_3^+, are now limited by the error limit for $\Delta_f H_0^0(CH_4)$.[21,22] In the case of CH_3X (X=Br and I), the maximum differences or discrepancies among their previously reported $\Delta_f H_{298}^0$ values are 1.7–3.3 kJ/mol.[3] These discrepancies are significantly larger than the error limit of 0.33 kJ/mol for $\Delta_f H_0^0(CH_3^+)$ derived in the previous PFI-PEPICO study of CH_4.[17] We show here that by measuring accurate 0 K AE(CH_3^+) values for reaction (1) using the PFI-PE and PFI-PEPICO method, we have obtained values for $\Delta_f H_0^0(CH_3X)$ with significantly improved precision,

$$CH_3X + h\nu \rightarrow CH_3^+ + X + e^-. \quad (1)$$

We have also re-examined the IE of CH_3Br using the PFI-PE method. By measuring the 0 K AE(CH_3^+) values for reaction (1) and IE of CH_3Br, together with the known IE of CH_3,[23] we have deduced highly precise D_0 values for CH_3–X and CH_3^+–X.

II. EXPERIMENT

The PFI-PE and PFI-PEPICO experiments were conducted using the high-resolution VUV photoelectron-photoion facility of the Chemical Dynamics Beamline at the Advanced Light Source (ALS).[12,24] The experimental procedures have been described in detail previously.[12–14,25,26] Thus, only a brief description is given here.

In the present experiment, Ar was used in the harmonic gas to filter higher undulator harmonics with photon energies greater than 15.76 eV. The ALS was operated in the multibunch mode with a period of 656 ns. The multibunch light structure consisted of 272 micro-VUV light pulses (pulse width=50 ps, separation of adjacent pulses=2 ns) followed by a dark gap (light off period) of 112 ns. A 2400 lines/mm grating (dispersion=0.64 Å/mm) was used to disperse the first order harmonic of the undulator VUV beam with entrance/exit slits set in the range of 30–100 μm. The resulting monochromatic VUV beam was then focused into the photoionization/photoexcitation (PI/PEX) center of the photoelectron-photoion apparatus. The photon energy ($h\nu$) calibration was achieved using the $Ar^+(^2P_{3/2})$, $Xe^+(^2P_{3/2})$, and $NO^+(X\,^1\Sigma^+, v^+=0)$ PFI-PE bands[27] recorded under the same experimental conditions before and after each scan. This calibration procedure assumes that the Stark shift for ionization thresholds of CH_3X and the rare gases and NO are identical. On the basis of previous experiments, the accuracy of the energy calibration is believed to be within ± 0.5 meV.[28]

The PFI-PE detection was achieved by employing the electron TOF scheme.[13] A dc field of 0.2 V/cm was main-

tained at the PI/PEX region to sweep background electrons formed by direct and prompt autoionization toward the electron detector prior to the application of the electric field pulse for Stark ionization. The PFI pulse (height=7.3 V/cm, width=200 ns) was applied ≈10 ns after the start of the dark gap. The PFI pulse also served to extract PFI-photoions toward the ion detector. Since the dark gap was only 112 ns in duration, a finite overlap occurred between the PFI pulse and micro light pulses of the subsequent period, resulting in the destruction of finite high-n Rydberg CH_3X molecules.

The ion PFI-PEPICO TOF spectra were recorded using a multichannel scaler triggered by the detection of PFI electrons.[14] The average accumulation time for a PFI-PEPICO TOF spectrum for CH_3X is ≈20 min. The current setup is sensitive to the ion kinetic energy.[14] The analysis of the Ar TOF peak obtained using a supersonic Ar beam reveals that the thermal background of Ar in the photoionization chamber contributes ≈15% to the experimental Ar sample. This 85:15 ratio is roughly consistent with the estimated CH_3X densities for the molecular beam sample and thermal background gas at the PI/PEX region. On the basis of the measured PFI-PE band for $Xe^+(^2P_{3/2})$, we estimate that the ion-energy selection achieved here is ≈1.0 meV (FWHM).[14]

The $CH_3Br(CH_3I)$ sample with a specified purity of 99% was obtained from Aldrich and used without further purification. All PFI-PEPICO TOF spectra for CH_3Br were recorded by introducing the CH_3Br sample into the PI/PEX region in the form of a skimmed neat CH_3Br supersonic beam (nozzle diameter=127 μm, stagnation pressure=760 Torr, and stagnation temperature=298 K). The vapor pressure for CH_3I at room temperature (298 K) is about 400 Torr. The vapor of a liquid CH_3I sample at 298 K was mixed with Ar to a total stagnation pressure of about 760 Torr prior to expansion through the nozzle. The PFI-PE spectra for CH_3X near their dissociation region were recorded using both the supersonic and effusive beam samples.

III. RESULTS AND DISCUSSION

A. PFI-PEPICO TOF spectra and breakdown diagrams for CH_3X

We have collected PFI-PEPICO TOF spectra for CH_3Br in the photon energy region of 12.68–12.89 eV, which is near the 0 K AE(CH_3^+) from CH_3Br. Figure 1(a) depicts typical PFI-PEPICO spectra of CH_3Br at selected photon energies, $h\nu$=10.5427, 12.7749, 12.8048, 12.8347, and 12.8556 eV. These spectra have been background corrected using procedures described in previous studies.[14] At photon energies well below the dissociation threshold, we measured the PFI-PEPICO TOF spectra at a step size of 10 meV, while a step size of 1.0 meV was used at photon energies close to the 0 K AE of reaction (1). The bottom TOF spectrum of Fig. 1(a) was recorded at the IE of CH_3Br with an accumulation time of 5 min. The fact that the photoion background at the

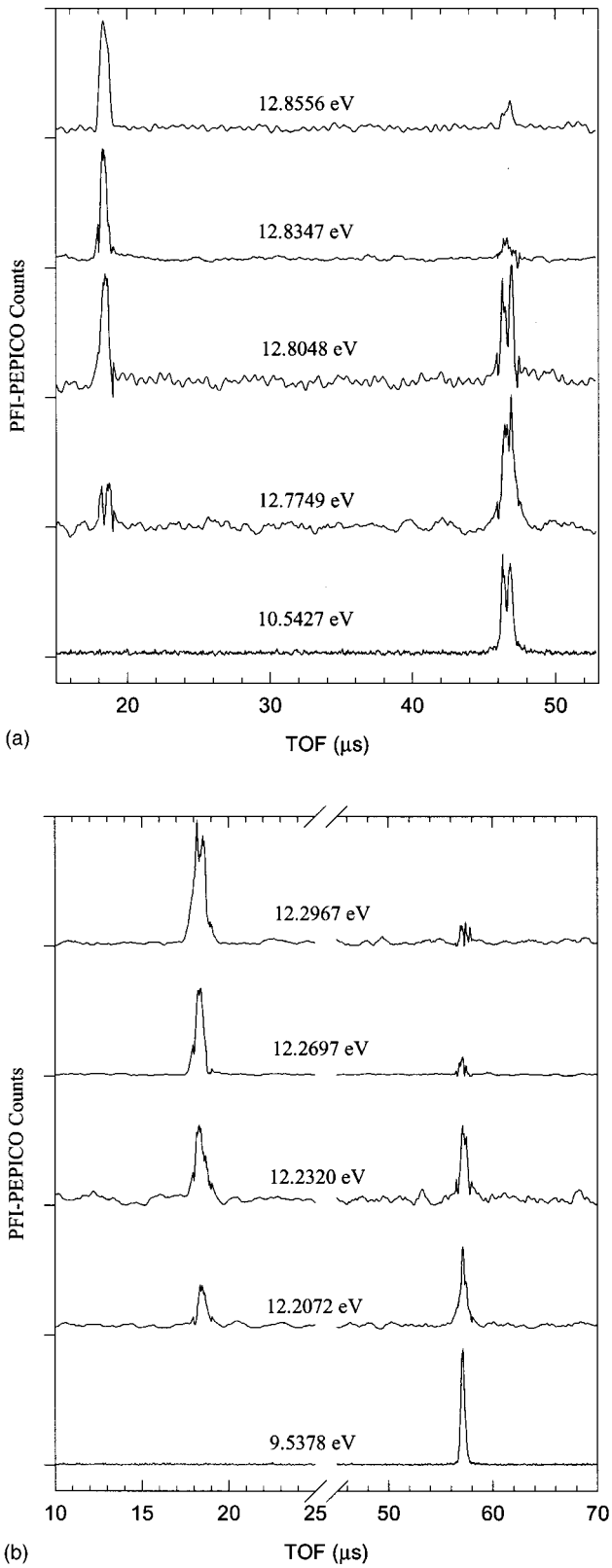

FIG. 1. (a) Selected PFI-PEPICO TOF spectra for CH_3^+ and CH_3Br^+ from CH_3Br at $h\nu$=10.5427, 12.7749, 12.8048, 12.8347, and 12.8556 eV. The TOF peak centered at 19.78 μs is due to CH_3^+, and the doublet peaks resolved at 46.32 and 46.84 μs are associated with $CH_3{}^{79}Br$ and $CH_3{}^{81}Br$, respectively. (b) PFI-PEPICO TOF spectra for CH_3^+ and CH_3I^+ from CH_3I at $h\nu$=9.5378, 12.2072, 12.2320, 12.2697, and 12.2967 eV. The TOF peaks centered at 19.78 and 57.12 μs are due to CH_3^+ and CH_3I^+, respectively.

TABLE I. Vibrational and rotational constants for CH_3Br and CH_3I.

	Vibrational frequencies (cm^{-1})[a]						Rotational constants (cm^{-1})[b]	
	$\nu_1(a)$	$\nu_2(a)$	$\nu_3(a)$	$\nu_4(e)$	$\nu_5(e)$	$\nu_6(e)$		
CH_3Br	2935	1306	611	3056	1443	955	5.08	0.3192
CH_3I	2933	1252	533	3060	1436	822	5.11	0.2502

[a]Reference 3.
[b]Reference 30.

IE is low results in excellent signal to noise (S/N) ratios for the PFI-PEPICO TOF data. As expected, this spectrum at $h\nu=10.5427$ eV only manifests the formation of parent CH_3Br ions. The TOF peak for the parent ion is resolved into a doublet at 46.32 and 46.84 μs, which can be assigned to ion masses of 94 and 96 amu. The relative intensities of the doublet reflect the nearly 1:1 natural isotopic distribution for ^{79}Br and ^{81}Br in CH_3Br^+. The deconvoluted TOF peaks for $CH_3{}^{79}Br^+$ and $CH_3{}^{81}Br^+$ have a peak width of 0.3 μs (FWHM). Other PFI-PEPICO TOF spectra taken at photon energies near the dissociation onset show poorer S/N ratios. The poorer S/N ratios for the PFI-PEPICO TOF spectra observed at $h\nu=12.7749$ and 12.8048 eV are also caused by the fact that these energies lie close to the Franck–Condon gap region of the photoelectron spectrum for CH_3Br.[29] Consequently, a significantly lower PFI-PE counts are observed in this region than those found at the IE of CH_3Br.

We have recorded PFI-PEPICO TOF spectra for CH_3I in the photon energy region of 12.15–12.32 eV. Selected spectra at $h\nu=9.5378$, 12.2072, 12.2320, 12.2697, and 12.2967 eV are depicted in Fig. 1(b). The bottom spectrum of Fig. 1(b), which was taken at the IE of CH_3I, shows the best S/N ratio compared to those for other spectra.

Table I lists the known vibrational frequencies for CH_3X.[3,30] Since these vibrational frequencies are relatively high, we expect that the thermal energy for CH_3X at 298 K due to vibrational excitation is small. The thermal vibrational energies for CH_3X molecules in the supersonic beam should be lower because their vibrational temperatures are expected to be <298 K. The average rotational energy for thermal CH_3X at 298 K amounts to $\approx 30-40$ meV. Assuming that all thermal rotational and vibrational energies are available to dissociation, we expect to observe daughter CH_3^+ ions below the 0 K AE for reaction (1). The daughter CH_3^+ ions observed in the PFI-PEPICO TOF spectra at $h\nu=12.7749$ and 12.8048 eV for CH_3Br and at $h\nu=12.2072$ and 12.2320 eV for CH_3I are due to dissociation of thermally excited parent molecules. This observation is consistent with the AEs measured below. As the photon energy is increased, the abundance for the parent ion decreases relative to that for the daughter ion.

At photon energies higher than the 0 K AE, complete dissociation should be observed. This is the case in the PFI-PEPICO studies of CH_4 and C_2H_2.[17,18] We showed that the 0 K AE for CH_3^+ from CH_4 (C_2H^+ from C_2H_2) can be determined unambiguously by the energy at which the intensity for the parent $CH_4^+(C_2H_2^+)$ ion goes to zero. However, in the PFI-PEPICO study of NH_3, we observed residual background coincidence intensities for the parent NH_3^+ ion peak at energies beyond the 0 K AE(NH_2^+).[16] An observation similar to the case of NH_3 is found here. As shown in Fig. 1(a) [1(b)], finite residual intensities for the parent $CH_3Br^+(CH_3I^+)$ ion peaks were found in the TOF spectra at $h\nu=12.8347$ and 12.8556 eV ($h\nu=12.2697$ and 12.2967 eV), which are shown (see discussion below) to be higher than the 0 K AE(CH_3^+) from CH_3Br (CH_3I). This observation can be attributed to coincidence background from hot electrons and dissociative photoionization of dimers and clusters formed in the supersonic beam. In the NH_3 and present experiment, the ALS dark gap (112 ns) is narrower than that (144 ns) used in the PFI-PEPICO studies of CH_4 and C_2H_2.[14,15] Thus, the contamination due to a finite dispersion of hot electrons into the dark gap in the present study is higher than that in the latter studies. The hot photoelectrons occurring at the dark gap are probably responsible for the majority of coincidence background associated with the detection of stable, cold parent ions. Under the conditions for supersonic expansion in the present experiment, we expect the formation of CH_3X dimers [$(CH_3X)_2$] and clusters in the beam sample. Stemming from the fact that the photon energy range of interest near the 0 K AE for reaction (1) is well above the IE of CH_3X, we expect the formation of CH_3X^+ from the dissociative photoionization process, such as reaction (2), to be a dominant channel,

$$(CH_3X)_2+h\nu\rightarrow CH_3X^++CH_3X+e^-. \tag{2}$$

In this reaction, CH_3X^+ is stabilized by the ejection of CH_3X. Thus, the PFI-PEPICO detection of reaction (2) may contribute to a finite coincidence background for CH_3X^+. Considering that the narrow photon energy range involved here, we also expect the cross section for reaction (2) to be independent of photon energy. The argument favoring a finite contribution to the coincidence background for CH_3X^+ by dissociative photoionization of dimers and clusters is consistent with the finding that the abundances for parent CH_4^+ and $C_2H_2^+$ are negligible at photon energies higher than their respective 0 K AEs because dimers and clusters for these species are not easily formed under the supersonic expansion conditions used in these experiments.

In order to construct the breakdown curves for the parent CH_3X^+ and daughter CH_3^+ ions, we first obtained the relative intensities for CH_3X^+ and CH_3^+ ions based on their respective TOF peak areas observed in the PFI-PEPICO TOF spectra. The fractional abundance for $CH_3X^+(CH_3^+)$ at a given photon energy was obtained by dividing the $CH_3X^+(CH_3^+)$ ion intensity by the sum of the CH_3X^+ and CH_3^+ ion intensities. These breakdown curves for CH_3X^+

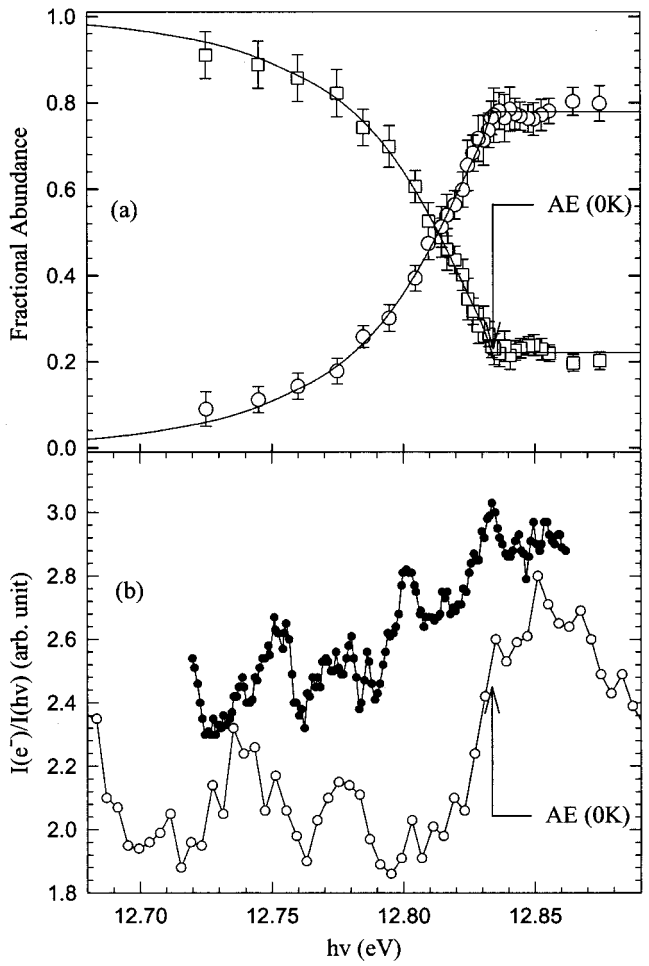

FIG. 2. (a) Breakdown curves for CH_3^+ (open circles) and CH_3Br^+ (open squares) from CH_3Br in the $h\nu$ range of 12.68–12.89 eV. The solid lines are simulations curves obtained by assuming 80% cold beam (20 K) and 20% thermal (298 K) CH_3Br sample. The error bars represent one standard deviation. The 0 K AE is marked by the break of the breakdown curve for the parent CH_3Br^+ ion. (b) PFI-PE spectra for CH_3Br in the range of 12.68–12.89 eV obtained using an effusive beam (solid circles, upper spectrum) and a supersonic beam (open circles, lower spectrum) sample of CH_3Br. The step at the 0 K AE is discernible in the cold (lower) PFI-PE spectrum.

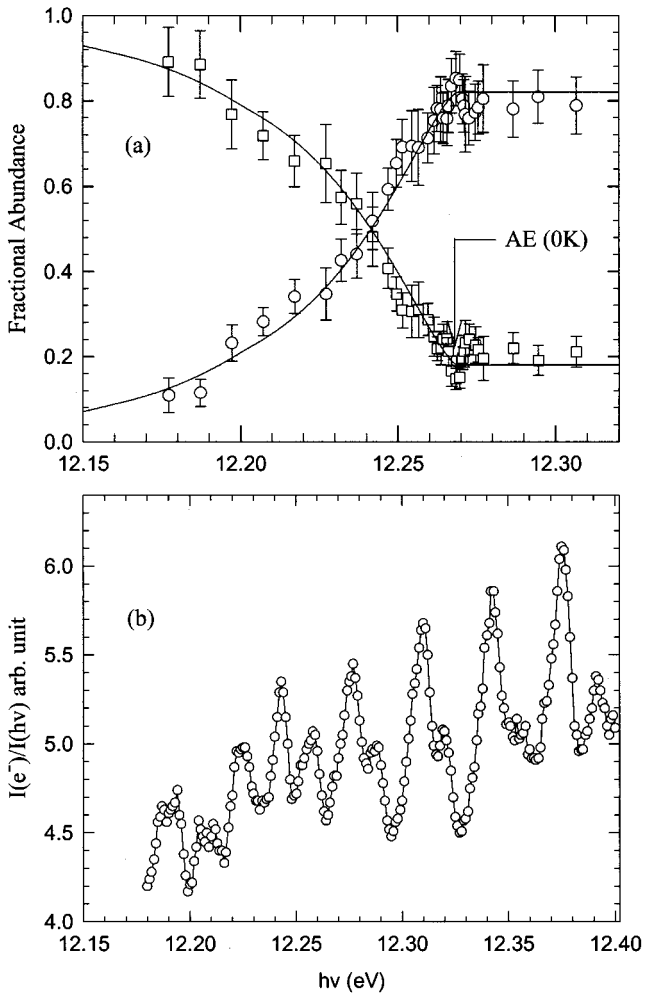

FIG. 3. (a) Breakdown curves for CH_3^+ (open circles) and CH_3I^+ (open squares) from CH_3I in the $h\nu$ range of 12.15–12.32 eV. The solid lines are simulations curves obtained by assuming a CH_3I sample at 298 K with no contribution from the cold sample. The error bars represent one standard deviations. The 0 K AE is marked by the break of the breakdown curve for CH_3I^+. (b) PFI-PE spectra for CH_3I in the range of 12.15–12.40 eV obtained using a supersonic beam of CH_3I. A step at the 0 K AE is not clearly discernible due to interference by the strong vibrational structure appearing in this region.

(open squares) and CH_3^+ (open circles) representing the plots of the fractional abundances for CH_3X^+ and CH_3^+ as a function of photon energy are shown in Fig. 2(a) for CH_3Br and in Fig. 3(a) for CH_3I. Error bars for individual data points shown in Figs. 2(a) and 3(a) represent their standard deviations.

As shown in Figs. 2(a) and 3(a), the fractional abundance for parent ion (daughter ion) decreases (increases) as the photon energy is increased. The distinct feature of the breakdown diagram for CH_3Br is the break observed at 12.834 eV, where the fractional abundance for $CH_3Br^+(CH_3^+)$ becomes a constant of 0.22 (0.78). The S/N ratios of the breakdown data for CH_3I are poorer than those for CH_3Br. A similar break is observed in breakdown diagram for CH_3I at 12.269 eV, where the fractional abundance for $CH_3I^+(CH_3^+)$ reaches a constant of 0.18 (0.82). Similar to the analysis of PFI-PEPICO data for NH_3, we have assigned the break of the breakdown curve of CH_3Br^+ at 12.834 $\pm$0.002 eV to be the 0 K AE(CH_3^+) from CH_3Br and that of CH_3I^+ at 12.269$\pm$0.003 eV to be the 0 K AE(CH_3^+) from CH_3I. The respective error ranges of 4 meV and 6 meV for the 0 K AE(CH_3^+) from CH_3Br and CH_3I are consistent with the simulation of the breakdown diagrams for CH_3X to be described in Sec. III B.

B. Simulation of the breakdown diagrams for CH_3X

The breakdown curves for CH_3X^+ and CH_3^+ were simulated by assuming that the ion energy resolution is infinitely narrow and that the broadening of the breakdown diagram is due solely to the thermal energy in the CH_3X molecule. The distribution of internal thermal energy $P(E,T)$,[16,19,20] was determined by Eq. (3), which depends on the density of the rovibrational states $\rho(E)$,

$$P(E,T)=\frac{\rho(E)e^{-E/RT}}{\int_0^\infty \rho(E)e^{-E/RT}}. \tag{3}$$

The density of rovibrational states for CH_3X was calculated using the Beyer–Swinehart direct count algorithm[31] based on the vibrational frequencies and rotational constants listed in Table I. The simulation were obtained by convoluting this thermal energy distribution with a step function at the 0 K AE as given by Eqs. (4) and (5),

$$\text{Parent}(h\nu) = \int_0^{\text{AE}-h\nu \text{ or } 0} P(E)dE, \tag{4}$$

$$\text{Daughter}(h\nu) = \int_{\text{AE}-h\nu \text{ or } 0}^{\infty} P(E)dE. \tag{5}$$

We note that the parent ion integral is valid only up to the $h\nu$ equal to the AE. Ideally, beyond that $h\nu$ value the parent ion signal is zero. The simulation of the breakdown curves also assumes a constant false coincidence background, resulting in a constant fractional abundance (0.22 for X=Br and 0.18 for X=I) for CH_3X^+ at $h\nu \geqslant$ AE. The breakdown data were fitted by two independent parameters, namely, the CH_3X temperature and the 0 K AE. The sample temperature governs the slope at which the 0 K AE is approached. If the sample temperature was 0 K and in the absence of thermal background gas in the chamber, the breakdown curves for CH_3X^+ and CH_3^+ would be a step function. Assuming the CH_3Br sample to consist of ≈20% thermal (298 K) background and ≈80% cold (20 K) beam sample, we have obtained an excellent simulation [solid lines, Fig. 2(a)] of the breakdown curves for CH_3Br^+ and CH_3^+, yielding a value of 12.834±0.002 eV for the 0 K AE(CH_3^+) from CH_3Br. In Fig. 3(a), the solid lines represent the simulated breakdown curves for CH_3I^+ and CH_3^+ calculated by assuming that the temperature for CH_3I is 298 K with little contribution from the cold beam sample. This simulation provides a value of 12.269±0.003 eV for the 0 K AE(CH_3^+) from CH_3I. As shown in previous study,[17] the detailed structure of breakdown curves derived from PFI-PEPICO measurements depends on the Stark field. Thus, the temperatures used in the simulation of the breakdown curves are not expected to reflect the actual temperatures of the gas sample involved.

We emphasize that the 0 K AE(CH_3^+) value determined here is based on the intrinsic feature, i.e., the break observed in the breakdown curve for CH_3X^+, and is not dependent on the detailed simulation of the breakdown curves. However, the successful simulation of the breakdown curves can be taken as support of the rationale for the AE assignment. In order to illustrate the precision of the present AE determination, we have plotted in Fig. 4 a magnified view of the breakdown data for CH_3Br^+ (open squares), together with their error bars (two standard deviations), in the photon energy region of 12.811–12.881 eV. The solid curve represents the best simulation curve. It is clear from this figure that the break (marked as 0 K AE by the arrow) of the CH_3Br^+ breakdown curve can be identified at 12.834 eV with an error limit better than ±3 meV. The assigned error limit of ±0.002 eV (± one standard deviation) is consistent with that obtained by simulation, which has taken into account the data fluctuation in the range bounded by the upper and lower dashed curves of Fig. 4.

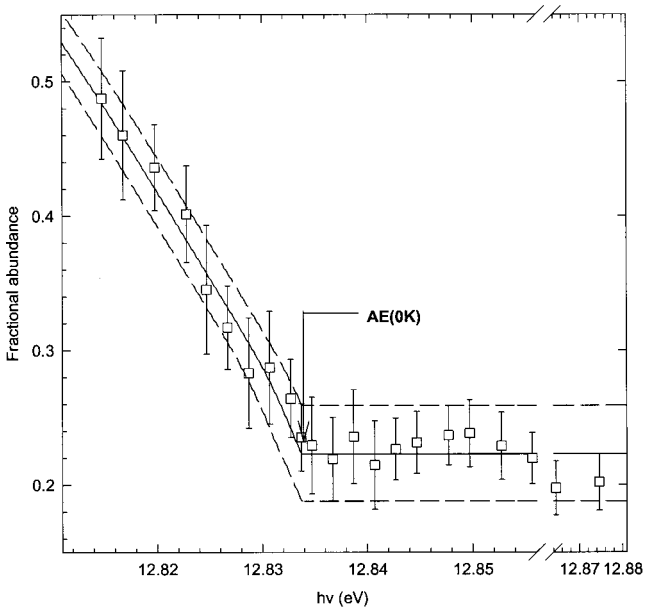

FIG. 4. A magnified view of the breakdown data for CH_3Br^+ (□) in the $h\nu$ range of 12.811–12.881 eV. The break resolved at 12.834 eV marks the 0 K AE(CH_3^+) from CH_3Br. The middle solid curve represents the best simulation curve. The assigned error limit of ±0.002 eV for the latter 0 K AE is consistent with that obtained by simulation, which has taken into account the data fluctuation in the range bounded by the upper and lower dashed curves.

C. PFI-PE spectra for CH_3X

The neutral $CH_3X(\tilde{X}\,^1A_1)$ ground state possesses C_{3v} symmetry and has the main electronic configuration $\cdots(1a_1)^2(2a_1)^2(1e)^4(3a_1)^2(2e)^4$.[29] The ejection of an electron from the highest occupied $2e$-orbital results in the formation of the ionic $CH_3X^+(\tilde{X}\,^2E)$ ground state. This state with the configuration $\cdots(2e)^3$ is subject to the Jahn-Teller vibronic distortion. However, to a first approximation, we can label the ground ionic state to consist of the spin–orbit components $CH_3X^+(\tilde{X}\,^2E_{3/2,1/2})$.[29]

The IE[$CH_3Br^+(\tilde{X}\,^2E_{3/2})$] measurements reported in previous photoionization,[32] photoelectron,[29] and spectroscopic[33] measurements are in excellent agreement with values mostly in the range of 10.53–10.54 eV. In order to obtain a more precise value for the IE of CH_3Br, we have measured the PFI-PE spectrum near the ionization onset of CH_3Br (not shown here). The spectrum was measured using an effusive CH_3Br beam with a step size of 0.5 meV. The PFI-PE resolution achieved was better than 1 meV (FWHM) as indicated by the PFI-PE peak for $Ar^+(^2P_{3/2})$. The PFI-PE bands for $CH_3Br^+(\tilde{X}\,^2E_{3/2,1/2})$ thus obtained exhibit a FWHM of ≈3–5 meV. Since the electron removed from the $2e$-orbital is a lone-pair electron associated with the Br atom and is not involved in bonding of CH_3Br,[29] the peak positions of the PFI-PE bands are expected to provide accurate measures for the IE[$CH_3Br^+(\tilde{X}\,^2E_{3/2,1/2})$] values. Based on the peak positions of the PFI-PE bands for $CH_3Br^+(\tilde{X}\,^2E_{3/2,1/2})$, we obtained IE[$CH_3Br^+(\tilde{X}\,^2E_{3/2})$] $=10.5427\pm0.0010$ eV and IE[$CH_3Br^+(^2E_{1/2})$]$=10.8615$ ±0.0010 eV.

The respective IE[$CH_3I^+(\tilde{X}\,^2E_{3/2})$] and

$IE[CH_3I^+(^2E_{1/2})]$ have been determined previously to be $76\,932\pm5\ cm^{-1}$ (9.5386 ± 0.0006 eV) and $81\,983\pm5\ cm^{-1}$ (10.1646 ± 0.0006 eV) in a nonresonant two photon (N2P) laser PFI-PE by Strobel *et al.*[34] These values are in excellent agreement with the values $IE[CH_3I^+(\tilde{X}\,^2E_{3/2})]=76\,930\pm1\ cm^{-1}$ (9.5381 ± 0.0001 eV) and $IE[CH_3I^+(^2E_{1/2})]=81\,979\pm1\ cm^{-1}$ (10.1641 ± 0.0001 eV) determined by the extrapolation of Rydberg series.[35] We have measured the PFI-PE bands for $CH_3I^+(\tilde{X}\,^2E_{3/2,1/2})$ and obtained values of $IE[CH_3I^+(\tilde{X}\,^2E_{3/2})]=9.5377\pm0.0010$ eV and $IE[CH_3I^+(^2E_{1/2})]=10.1639\pm0.0010$ eV. The fact that these latter measurements are in excellent agreement with results of the previous N2P-PFI-PE and Rydberg series extrapolation studies indicates that the $IE[CH_3Br^+(\tilde{X}\,^2E_{3/2,1/2})]$ values determined here are highly reliable.

Figure 2(b) shows the PFI-PE spectra for CH_3Br in the energy region of 12.68–12.89 eV obtained using an effusive sample (upper spectrum, solid circles) and a supersonic beam sample (lower spectrum, solid circles) of CH_3Br. This energy region covers the 0 K $AE(CH_3^+)$ from CH_3Br. In the previous PFI studies, sharp steps were found in the PFI-PE spectra for CH_4, C_2H_2, and NH_3, marking precisely the corresponding 0 K AEs for CH_3^+, C_2H^+, and NH_2^+ determined in PFI-PEPICO measurements.[15–18] A detailed discussion concerning the conditions for the observation of a step at the 0 K ion dissociation threshold has been given previously.[15,16] As shown in Fig. 2(b), the PFI-PE spectra for CH_3Br are highly structured, consisting of complex vibrational bands for the $CH_3Br^+(\tilde{A}\,^2A_1)$ state.[29] Although the PFI-PE spectrum obtained using an effusive CH_3Br sample at 298 K shows a general increase in PFI-PE intensity as the photon energy is increased, a step at the 0 K $AE(CH_3^+)$ is not discernible. Comparing the PFI-PE spectra using effusive and supersonic beam, we can clearly identify a sharp step at the 0 K $AE(CH_3^+)$ as marked in Fig. 2(b). This observation is a confirmation for the 0 K $AE(CH_3^+)=12.834\pm0.002$ eV determined in the PFI-PEPICO TOF study of CH_3Br.

In accordance with the conclusion of previous studies,[15–18] the formation of CH_3^+ from CH_3Br in the present PFI experiment is believed to proceed via processes 6(a), 6(b), and 6(d) at energies slightly above the $AE(CH_3^+)$, while CH_3Br^+ ions are produced by processes 6(a) and 6(c) below the $AE(CH_3^+)$,

$$\begin{array}{ccccc} & \text{(a)} & & \text{(b)} & \\ CH_3Br+h\nu & \rightarrow & CH_3Br^* & \rightarrow & CH_3^*+Br \\ & & \downarrow\text{(c)} & & \downarrow\text{(d)} \\ & & CH_3Br^{+*}+e^- & & CH_3^++e^-. \end{array} \quad (6)$$

Here, CH_3Br^* and CH_3^* represent excited CH_3Br and CH_3, respectively, in long-lived high-n ($n\geqslant100$) Rydberg states and CH_3Br^{+*} stands for internally excited CH_3Br^+. Processes 6(c) and 6(d) are PFI processes. This mechanism suggests that CH_3Br^* fragments into CH_3^*+Br at energies above the $AE(CH_3^+)$ prior to the PFI process 6(d) and is responsible for the sharp step at 12.834 eV observed in the cold beam PFI-PE spectrum of CH_3Br shown in Fig. 2(b).

The dominant decay channels for CH_3Br^* are autoionization and fragmentation. At energies below the $AE(CH_3^+)$, the PFI-PE signal is due to process 6(c) and is proportional to the concentration of CH_3Br^* species that have survived the decay for a time longer than the delay ($\Delta\tau\approx10^{-1}$ s) of the PFI pulse relative to the excitation VUV light pulse. For CH_3Br^* species that have spontaneously autoionized at a time shorter than $\Delta\tau$ are lost to PFI detection. The CH_3^* species formed at the AE are expected to converge to the ground state of CH_3^+, i.e., below the IE of CH_3. Consequently, autoionization is not accessible to CH_3^* fragments. The CH_3^* fragments produced at energies slightly above the AE can only autoionize by rotational autoionization. The latter process is expected to be slower than vibrational and electronic autoionization for the case of CH_3Br^*, which lies well above the IE of CH_3Br. Assuming that the decay rates via fragmentation for CH_3Br^* and CH_3^* are similar, we expect that a larger fraction of CH_3^* survives the decay than that of CH_3Br^*. This explains why the PFI-PE signals derived from process 6(d) at photon energies slightly above the AE are higher than that observed below the AE. The observation of the sharp step feature in the PFI-PE spectrum is consistent with the conclusion that the conversion from CH_3Br^* to CH_3^* is complete prior to process 6(d) and that the dissociation process has a rate constant $\gg1/\Delta\tau$ ($\approx10^7\ s^{-1}$).[15,16]

As pointed out above, the dissociation leading to the production of CH_3^* from CH_3Br^* formed by VUV excitation of thermally excited CH_3Br molecules occurs below the 0 K AE. As a result of the magnification of PFI events for CH_3^* fragments, the PFI-PE spectrum observed using an effusive beam of CH_3Br [upper spectrum in Fig. 2(b)] is expected to manifest a higher nominal temperature than the actual temperature of the thermal CH_3Br sample. This would result in the efficient filling of the step in the PFI-PE spectrum. This analysis indicates that the step occurring at the 0 K AE of a dissociative photoionization process is more readily identified using a cold sample.

The PFI-PE spectrum for CH_3I in the region of 12.15–12.40 eV measured using a supersonic CH_3I beam sample is shown in Fig. 3(b). This spectrum reveals strong vibrational PFI-PE bands for the $CH_3I^+(\tilde{A}\,^2A_1)$ state, which is formed by the removal of an electron from the $3a_1$-orbital in the $CH_3X(\tilde{X}\,^1A_1)$ state.[29] These vibrational bands have been observed and assigned previously to excitations of the umbrella mode (ν_2) and C–I stretching mode (ν_3) of $CH_3I^+(\tilde{A}\,^2A_1)$.[36] The excitation of these modes is to be expected considering that the $3a_1$-orbital has predominantly C–I bonding character. The step expected at the 0 K $AE(CH_3^+)$ [marked in Fig. 3(a)] coincides with the rising edge of a strong vibrational PFI-PE peak, and thus cannot be identified. The previous threshold photoelectron-photoion coincidence (TPEPICO) study[37] indicated that the dissociation rate of CH_3I^+ is slow near threshold with a value of $\approx10^7\ s^{-1}$. Thus, a step might not be observable in the PFI-PE spectrum of CH_3I.

TABLE II. Comparison of values for ionization energies (IEs) of CH_3Br and CH_3, 0 K heats of formation ($\Delta_f H_0^0$) for CH_3Br, CH_3Br^+, CH_3, and CH_3^+, 0 K AE for CH_3^+[AE(CH_3^+)] from CH_3Br, and 0 K bond dissociation energies (D_0's) for CH_3–Br and CH_3^+–Br.

AE(CH_3^+) (eV)	IE(eV)		$\Delta_f H_0^0$ (kJ/mol)[a]				D_0 (eV)[b]	
	CH_3Br	CH_3	CH_3Br	CH_3Br^+	CH_3	CH_3^+	CH_3–Br	CH_3^+–Br
12.834±0.002[b]	**10.5427±0.0010**[c] **[10.8615±0.0010]**[c]	**9.8380±0.0004**[d]	**−21.30±0.42**[b] **(−36.36±0.42)**[b]	**995.88±0.42**[b] **(981.52±0.42)**[b]	**149.83±0.33**[e] **(147.23±0.33)**[e]	**1099.05±0.33**[f] **(1095.62±0.33)**[f]	**2.996±0.002**	**2.291±0.002**
12.77[g]	10.541±0.003[i]	9.84±0.01[k]	−23.0±1.3[m] (−38.1±1.3)[m]					
12.80±0.03[h]	10.54±0.01[h]	9.843±0.002[l]	−19.24±0.84[n] (−34.31±0.84)[n]					
	10.53[j]		−22.5±1.5[o,p] (−37.5±1.5)[p] −22.6±1.3[o,p] (−37.7±1.3)[p]					
G2/G3 predictions[q]								
12.75/12.83	10.62/10.63	9.77/9.85	−14.6/−19.2 (−29.7/−34.3)	1009.6/1006.7 (995.4/992.0)	154.8/149.8 (152.3/146.9)	1097.0/1100.4 (1093.7/1097.0)	2.98/2.97	2.13/2.20

[a]The values in parentheses are $\Delta_f H_{f298}^0$ values converted from $\Delta_f H_0^0$ values. See the text.
[b]This work.
[c]The upper value is IE[$CH_3Br^+(\tilde{X}\,^2E_{3/2})$]. The value in square bracket is IE[$CH_3Br^+(^2E_{1/2})$].
[d]Reference 23.
[e]References 17 and 23.
[f]Reference 17.
[g]Reference 38.
[h]Reference 32.
[i]Reference 33.
[j]Reference 29.
[k]Reference 3.
[l]Reference 39.
[m]Reference 2.
[n]Reference 40.
[o]The $\Delta_f H_{f0}^0$ value is converted from $\Delta_f H_{f298}^0$ value.
[p]Reference 41.
[q]References 5 and 6.

D. Thermochemistry of the CH_3X/CH_3X^+ system

We have listed in Table II selected experimental[3,17,23,29,32,33,38–41] and theoretical[6] values for the IEs of CH_3Br and CH_3, $\Delta_f H_0^0$'s of CH_3Br, CH_3Br^+, CH_3, and CH_3^+, 0 K AE for CH_3^+ from CH_3Br, and D_0's for CH_3–Br and CH_3^+–Br. The 0 K AE(CH_3^+)=12.834±0.002 eV obtained here is higher than the literature values determined by PIE measurements,[32,40] which are in the range of 12.77–12.80 eV. The latest NIST compilation recommended a value of 10.541±0.003 eV for the IE of CH_3Br[3], which is in excellent accord with the IE[$CH_3Br^+(\tilde{X}\,^2E_{3/2})$] value of 10.5427±0.0010 eV determined in the present study. The IE[$CH_3Br^+(\tilde{X}\,^2E_{3/2})$] and 0 K AE($CH_3^+$) from CH_3Br determined here give the $D_0(CH_3^+–Br)$=2.291±0.002 eV. Combining the 0 K AE(CH_3^+) from CH_3Br and the known IE for CH_3 obtained in a previous PFI-PE study,[23] we calculate a value of 2.996 ±0.002 eV for $D_0(CH_3–Br)$.

The 0 K AE(CH_3^+) from CH_4 was determined to be 14.323±0.001 eV (1381.975±0.084 kJ/mol) in a previous PFI-PEPICO study.[17] Using the latter value, together with the known $\Delta_f H_0^0(CH_4)=-66.90\pm0.33$ kJ/mol) (Ref. 21) and $\Delta_f H_0^0(H)=216.020\pm0.004$ kJ/mol,[21] we have obtained $\Delta_f H_0^0(CH_3^+)=1099.05\pm0.33$ kJ/mol.[17] We note that the precision of this $\Delta_f H_0^0(CH_3^+)$ value is limited mainly by the error limit for $\Delta_f H_0^0(CH_4)$. The $\Delta_f H_0^0(Br)=117.93\pm0.13$ kJ/mol (Refs. 3 and 21) is also well known. Combining these values for $\Delta_f H_0^0(Br)$ and $\Delta_f H_0^0(CH_3^+)$ and the 0 K AE(CH_3^+) from CH_3Br determined here, we obtained a value of −21.30±0.42 kJ/mol for $\Delta_f H_0^0(CH_3Br)$. The NIST WebBook[3] lists three experimental $\Delta_f H_{298}^0(CH_3Br)$ values: −37.7±1.3, −37.5±1.5, and −34.31±0.84 kJ/mol.[40,41] Using the known vibrational frequencies for CH_3Br, we have converted these values to $\Delta_f H_0^0(CH_3Br)$ values of −22.6±1.3, −22.18±1.5, and −19.25±0.84 kJ/mol, respectively. The present value $\Delta_f H_0^0(CH_3Br)=-21.30\pm0.42$ kJ/mol lies in the range of previous experimental measurements,[38,39] and has a lower error limit than those for the latter values.

We have listed in Table III selected experimental[34,35,37,42–45] and theoretical[5,6] values for the IEs of CH_3I, $\Delta_f H_0^0$'s for CH_3I and CH_3I^+, 0 K AE(CH_3^+) from CH_3I, D_0's for CH_3–I and CH_3^+–I. The previous PIE (Refs. 38 and 42) and TPEPICO (Ref. 37) studies yield values in the range of 12.18–12.260 eV for the 0 K AE(CH_3^+) from CH_3I. The present value AE(CH_3^+)=12.269±0.003 eV lies on the high energy side of these values. In view of the excellent agreement between results obtained in the spectroscopic and N2P-PFI-PE studies,[34,35] we consider that the IE values for the formation of $CH_3I^+(\tilde{X}\,^2E_{3/2,1/2})$ from

TABLE III. Comparison of values for ionization energies of CH_3I, 0 K heats of formation ($\Delta_f H_0^0$) for CH_3I and CH_3I^+, CH_3, and 0 K AE for CH_3^+ [$AE(CH_3^+)$] from CH_3I, and and 0 K bond dissociation energies (D_0's) for CH_3–I and CH_3^+–I.

$AE(CH_3^+)$ (eV)	IE (eV)[a] CH_3I	$\Delta_f H_0^0$ (kJ/mol)[b]		D_0 (eV)[c]	
		CH_3I	CH_3I^+	CH_3–I	CH_3^+–I
2.269±0.003	**9.5381±0.0001**[d]	**22.43±0.50**[c]	**941.11±0.50**[e]	**2.431±0.003**	**2.731±0.003**
	[10.1641±0.0001][d]	**(13.22±0.50)**[c]	**(932.66±0.50)**[e]		
12.24±0.01[f]	9.5377±0.0010[c]	23.5±1.4[ij]			
	[10.1639±0.0010][c]	(14.3±1.4)[i]			
12.18[g]	9.5386±0.0006[h]	23.8±1.0[j,k]			
	[10.1646±0.0006][h]	(14.6±1.0)[j]			
12.260±0.013[i]		25.1±1.3[j,m]			
		(15.9±1.3)[m]			
G2 predictions[n]					
12.17	9.74	30.5	970.3	2.40	2.43
		(21.3)	(961.9)		

[a]The upper value is IE[$CH_3I^+(X\,^2E_{3/2})$], and the value in square bracket is IE[$CH_3I^+(^2E_{1/2})$].
[b]The values in parentheses are $\Delta_f H_{f298}^0$ values converted from $\Delta_f H_0^0$ values. See the text.
[c]This work.
[d]Reference 35.
[e]Obtained by combining the IE of Ref. 35 and $\Delta_f H_0^0$ determined in the present study.
[f]Reference 37.
[g]Reference 38.
[h]Reference 34.
[i]Reference 43.
[j]The $\Delta_f H_{f0}^0$ value is converted from the $\Delta_f H_{f298}^0$ value.
[k]Reference 44.
[l]Reference 42.
[m]Reference 45.
[n]Reference 5.

$CH_3I(\tilde{X}\,^1A_1)$ are well known. The more precise spectroscopic determinations,[35] $IE[CH_3I^+(\tilde{X}\,^2E_{3/2})]=9.5381\pm0.0001$ eV and $IE[CH_3I^+(^2E_{1/2})]=10.1641\pm0.0001$ eV, are recommended here. Using the known $\Delta_f H_0^0(I)=107.165\pm0.042$ kJ/mol,[22] $\Delta_f H_0^0(CH_3^+)=1099.05\pm0.33$ kJ/mol,[17] and the 0 K $AE(CH_3^+)$ of 1183.78 ±0.29 kJ/mol (12.269±0.003 eV) from CH_3I, we calculated a value $\Delta_f H_0^0(CH_3I)=22.43\pm0.50$ kJ/mol. We have converted this value into $\Delta_f H_{298}^0(CH_3I)=13.22\pm0.05$ kJ/mol. Three experimental values,[43–45] 14.3±1.4, 14.6±1.0, and 15.9±1.3 kJ/mol, are listed in the NIST WebBook[3] for $\Delta_f H_{298}^0(CH_3I)$. Taking into account the experimental uncertainties, the present result is in agreement with the value $\Delta_f H_{298}^0(CH_3I)=14.3\pm1.4$ kJ/mol obtained by Golden *et al.*[43]

The best or most precise energetic data for the CH_3/CH_3^+, CH_3Br/CH_3Br^+, and CH_3I/CH_3I^+ systems are highlighted in bold font in Tables II and III. These energetic data, including IEs, 0 K AEs, $\Delta_f H_0^0$'s and D_0's with error limits ≤0.50 kJ/mol, for CH_3/CH_3^+ and CH_3Br/CH_3Br^+ and CH_3I/CH_3I^+ obtained in the present and previous PFI-PE and PFI-PEPICO measurements should provide a challenge for state-of-the-art *ab initio* computational quantum theories. We have compared the most precise experimental values with G2/G3 predictions[5,6] in Tables II and III. The G3 predictions for the CH_3Br/CH_3Br^+ system are calculated using the new basis set for Br provided by Curtiss *et al.*[46] and are generally in better agreement with the experimental results than the G2 predictions. However, the G3 prediction for the IE of CH_3Br shows no significant improvement over the G2 prediction. The maximum deviations of 13.8 and 10.9 kJ/mol are observed for the respective G2 and G3 predictions for $\Delta H_{f0}^0(CH_3Br^+)/\Delta H_{f298}^0(CH_3Br^+)$. These errors are greater than the targeted errors of the G2/G3 computational procedures.[5,6] The larger errors observed here are caused by involvement of the heavy elements X=Br and I in CH_3X/CH_3X^+. At present, G3 calculations cannot be made for iodine-containing compounds. We have only computed the G2 predictions for the IE, 0 K AE, $\Delta_f H_0^0$, and D_0 for the CH_3I/CH_3I^+ system. As expected, the G2 predictions for CH_3I/CH_3I^+ are considerably poorer than those for CH_3Br/CH_3Br^+. The discrepancies between G2 predictions and the most precise experimental data for CH_3I/CH_3I^+ as shown in Table III are in the range of 2.9–29.3 kJ/mol.

IV. CONCLUSIONS

We have performed a high-resolution energy-selected study on the unimolecular dissociation reaction, $CH_3X^+\rightarrow CH_3^+ + X$, using the PFI-PE and PFI-PEPICO methods. The 0 K $AE(CH_3^+)$ from CH_3X and IE value for CH_3Br obtained in the present study, together with well known energetic data for Br, I, CH_3, CH_3^+, and CH_3I, have made possible the determination of more precise $\Delta_f H_0^0$ and D_0 values for CH_3X and CH_3X^+. This study shows that using the PFI-PE and PFI-PEPICO methods, highly reliable $\Delta_f H_0^0$ values for a range of neutral species can be determined to a precision comparable to those achieved for some of the most well known $\Delta_f H_0^0$ values reported in the literature, such

as $\Delta_f H_0^0(CH_4)$. The comparison of the best experimental energetic data for the CH_3X/CH_3X^+ system with G2/G3 predictions indicates that the G2/G3 values have errors up to 29.3 kJ/mol. We believe that energetic data such as those presented here with significantly smaller error limits compared to current literature values would play an important role in the development of the next generation of quantum chemical computation schemes.

ACKNOWLEDGMENTS

This work was supported by the Director, Office of Energy Research, Office of Basic Energy Sciences, Chemical Science Division of the U.S. Department of Energy under Contract No. W-7405-Eng-82 for the Ames Laboratory and Contract No. DE-AC03-76SF00098 for the Lawrence Berkeley National Laboratory. One of the authors (Y.S.) is the recipient of the Wall Fellowship in 1999 and the Henry Gilman Fellowship in 2000 at Iowa State University. One of the authors (C.Y.N.) acknowledges helpful discussions with Professor Tomas Baer.

[1] H. M. Rosenstock, M. K. Draxl, B. W. Steiner, and J. T. Herron, J. Phys. Ref. Data Suppl. **6** (Suppl. 1) (1977).
[2] S. G. Lias, J. E. Bartmess, J. L. Holmes, R. D. Levin, and W. G. Mallard, J. Phys. Chem. Ref. Data Suppl. **17**, 1 (1988).
[3] The NIST Chemistry WebBook, http://webbook.nist.gov/chemistry/
[4] J. Berkowitz, *Photoabsorption, Photoionization, and Photoelectron Spectroscopy* (Academic, New York, 1979).
[5] L. A. Curtiss, K. Raghavachari, G. W. Trucks, and J. A. Pople, J. Chem. Phys. **94**, 7221 (1991); M. N. Glukhovtsev, A. Pross, M. P. McGrath, and L. Radom, *ibid.* **103**, 1878 (1995).
[6] L. A. Curtiss, K. Raghavachari, P. C. Redfern, V. Rassolov, and J. A. Pople, J. Chem. Phys. **109**, 7764 (1998).
[7] K. Müller-Dethlefs, M. Sander, and E. W. Schlag, Z. Naturforsch. Teil A **39A**, 1089 (1984).
[8] E. W. Schlag, *ZEKE Spectroscopy* (Cambridge University Press, Cambridge, 1998).
[9] *High Resolution Laser Photoionization and Photoelectron Studies*, Wiley Series in Ion Chemistry and Physics, edited by I. Powis, T. Baer, and C. Y. Ng (Wiley, Chichester, 1995).
[10] P. M. Johnson, in *Photoionization and Photodetachment*, edited by C. Y. Ng (World Scientific, Singapore, 2000), Adv. Ser Phys. Chem., Vol. 10A, pp. 296–346.
[11] D. D. Martin and J. W. Hepburn, Phys. Rev. Lett. **79**, 3154 (1997); J. Chem. Phys. **109**, 8139 (1998).
[12] C. Y. Ng, in *Photoionization, and Photodetachment*, edited by C. Y. Ng (World Scientific, Singapore, 2000), Adv. Ser Phys. Chem. **10A**, Chap. 9, pp. 394–538.
[13] G. K. Jarvis, Y. Song, and C. Y. Ng, Rev. Sci. Instrum. **70**, 2615 (1999).
[14] G. K. Jarvis, K.-M. Weitzel, M. Malow, T. Baer, Y. Song, and C. Y. Ng, Rev. Sci. Instrum. **70**, 3892 (1999).
[15] K.-M. Weitzel, G. Jarvis, M. Malow, T. Baer, Y. Song, and C. Y. Ng, Phys. Rev. Lett. **86**, 3526 (2001).
[16] Y. Song, X.-M. Qian, K.-C. Lau, C. Y. Ng, J. Liu, and W. Chen, J. Chem. Phys. **115**, 2582 (2001).
[17] Karl-Michael Weitzel, Marcus Malow, G. K. Jarvis, Tomas Baer, Y. Song, and C. Y. Ng̃, J. Chem. Phys. **111**, 8267 (1999).
[18] G. K. Jarvis, Karl-Michael Weitzel, Marcus Malow, Tomas Baer, Y. Song, and C. Y. Ng, Phys. Chem. Chem. Phys. **1**, 5259 (1999).
[19] T. Baer, Y. Song, C. Y. Ng, J. Liu, and W. Chen, Faraday Discuss. **115**, 137 (2000).
[20] T. Baer, Y. Song, C. Y. Ng, W. Chen, and J. Liu, J. Phys. Chem. **104**, 1959 (2000).
[21] *JANAF Thermochemical Tables* (Dow Chemical, Midland, MI, 1977); J. Phys. Chem. Ref. Data **11**, 695 (1982).
[22] V. P. Glushko, L. V. Gurvich, G. A. Bergman, I. V. Veits, V. A. Medvedev, G. A. Khachkunuzov, and V. S. Yungman, *Termodinamicheski Svoistva Individual'nikh Veshchestv* (Nauka, Moscow, 1978), Vol. I, Books 1 and 2.
[23] J. A. Blush, P. Chen, R. T. Wiedmann, and M. G. White, J. Chem. Phys. **98**, 3557 (1993).
[24] P. Heimann, M. Koike, C.-W. Hsu, D. Blank, X. M. Yang, A. Suits, Y. T. Lee, M. Evans, C. Y. Ng, C. Flaim, and H. A. Padmore, Rev. Sci. Instrum. **68**, 1945 (1997).
[25] C.-W. Hsu, M. Evans, P. A. Heimann, and C. Y. Ng, Rev. Sci. Instrum. **68**, 1694 (1997).
[26] C.-W. Hsu, M. Evans, S. Stimson, C. Y. Ng, and P. Heimann, Chem. Phys. **231**, 121 (1998).
[27] G. K. Jarvis, M. Evans, C. Y. Ng, and K. Mitsuke, J. Chem. Phys. **111**, 3058 (1999).
[28] S. Stimson, Y.-J. Chen, M. Evans, C.-L. Liao, C. Y. Ng, C.-W. Hsu, and P. Heimann, Chem. Phys. Lett. **289**, 507 (1998).
[29] K. Kimura, S. Katsumata, Y. Achiba, T. Yamazaki, and S. Iwata, *Handbook of He I Photoelectron Spectra of Fundamental Organic Compounds* (Japan Scientific Society, Tokyo, 1981).
[30] G. Herzberg, *Molecular Spectra and Molecular Structure, Vol. III, Electronic spectra and Electronic structure of Polyatmoic Molecules* (Van Nostrand, New York, 1966).
[31] T. Beyer and D. F. Swinehart, Assoc. Comput. Mach., Commun. **16**, 379 (1973).
[32] B. P. Tsai, T. Baer, A. S. Werner, and S. F. Lin, J. Phys. Chem. **79**, 570 (1975).
[33] P. Hochmann, P. H. Templet, H.-T. Wang, and S. P. McGlynn, J. Chem. Phys. **62**, 2588 (1975); W. C. Price, *ibid.* **4**, 539 (1936).
[34] A. Strobel, A. Lochschmidt, I. Fischer, G. Niedner-Schatteburg, and V. E. Bondybey, J. Chem. Phys. **99**, 733 (1993); A. Strobel, I. Fischer, and A. Lochschmidt, J. Phys. Chem. **98**, 2024 (1994).
[35] M. A. Baig, J. P. Connerade, J. Dagata, and S. P. McGlynn, J. Phys. B **14**, L25 (1981).
[36] K. Walter, R. Weinkauf, U. Boesl, and E. W. Schlag, J. Chem. Phys. **89**, 1914 (1988).
[37] D. M. Mintz and T. Baer, J. Chem. Phys. **65**, 2407 (1976).
[38] M. Krauss, J. A. Walker, and V. H. Dibeler, J. Res. Natl. Bur. Stand., Sect. A **72A**, 281 (1968); J. C. Traeger and R. G. McLoughlin, J. Am. Chem. Soc. **103**, 3647 (1981).
[39] J. Berkowitz, G. B. Ellison, and D. Gutman, J. Phys. Chem. **98**, 2744 (1994).
[40] K. C. Ferguson, E. N. Okafo, and E. Whittle, J. Chem. Soc., Faraday Trans. 1 **69**, 295 (1973).
[41] G. P. Adams, A. S. Carson, and P. G. Laye, Trans. Faraday Soc. **62**, 1324 (1965); P. Fowell, J. R. Lacher, and J. D. Park, *ibid.* **61**, 1324 (1965).
[42] A. J. C. Nickolson, in *Recent Developments in Mass Spectrometroscopy*, edited by K. Ogata and T. Hayakawa (University Park, Baltimore, 1970), p. 745.
[43] D. M. Golden, R. Walsh, and S. W. Benson, J. Am. Chem. Soc. **87**, 4053 (1965).
[44] J. D. Cox and G. Pilcher, *Thermochemistry of Organic and Organometallic Compounds* (Academic, New York, 1965).
[45] C. A. Goy and H. O. Pritchard, J. Phys. Chem. **69**, 3040 (1965).
[46] L. A. Curtiss, P. C. Redfern, V. Rassolov, G. Kedziora, and J. A. Pople, J. Chem. Phys. **114**, 9287 (2001).